Development 134, 2261-2271 (2007) doi:10.1242/dev.02856

The role of Dpp and its inhibitors during eggshell patterning in *Drosophila*

Bhupendra V. Shravage, Gabriela Altmann, Martin Technau and Siegfried Roth*

The *Drosophila* eggshell is patterned by the combined action of the epidermal growth factor [EGF; Gurken (Grk)] and transforming growth factor β [TGF-β; Decapentaplegic (Dpp)] signaling cascades. Although Grk signaling alone can induce asymmetric gene expression within the follicular epithelium, here we show that the ability of Grk to induce dorsoventral polarity within the eggshell strictly depends on Dpp. Dpp, however, specifies at least one anterior region of the eggshell in the absence of Grk. Dpp forms an anteriorposterior morphogen gradient within the follicular epithelium and synergizes with the dorsoventral gradient of Grk signaling. High levels of Grk and Dpp signaling induce the operculum, whereas lower levels of both pathways induce the dorsal appendages. We provide evidence that the crosstalk between both pathways occurs at least at two levels. First, Dpp appears to directly enhance the levels of EGF pathway activity within the follicular epithelium. Second, Dpp and EGF signaling collaborate in controlling the expression of Dpp inhibitors. One of these inhibitors is *Drosophila sno* (*dSno*), a homolog of the Ski/Sno family of vertebrate proto-oncogenes, which synergizes with *daughters against dpp* and *brinker* to set the posterior and lateral limits of the region, giving rise to dorsal follicle cells.

KEY WORDS: Oogenesis, Follicle cells, EGF signaling, Gurken, Proto-oncogene, *dSno*, *brinker*, *Drosophila*

INTRODUCTION

The deposited *Drosophila* egg has a clear axial organization that is apparent from the overall shape of the egg and the presence of several prominent structures within the inner (vitelline membrane) and outer (chorion) eggshell (Spradling, 1993; Dobens and Raftery, 2000; Berg, 2005). The anterior egg pole is marked by a micropyle required for sperm entry, and the dorsal-anterior side of the egg carries the dorsal appendages (DAs) with a respiratory function and the operculum, a lid-like structure that opens when the larva hatches. The eggshell layers are secreted by the somatically derived follicle cells.

Two major signaling pathways control the specification of the dorsal chorion structures: the epidermal growth factor (EGF)- and the transforming growth factor β (TGF-β)-pathway (Nilson and Schupbach, 1999; Twombly et al., 1996; Dobens et al., 2000; Peri and Roth, 2000; Roth, 2003; Berg, 2005). The EGF/TGF-α-like ligand Gurken (Grk) (Neuman-Silberberg and Schupbach, 1993) is produced at the dorsal-anterior cortex of the oocyte where *grk* mRNA is localized. From this position Grk protein is secreted and activates the *Drosophila* EGF receptor (Egfr) in overlying dorsal follicle cells. These cells later produce the operculum and the two DAs.

Whereas Grk signaling also spreads to more posterior regions of the follicular epithelium, the operculum and DAs are only derived from anterior follicle cells. This restriction depends on a second, anterior signal that is likely to be provided by Decapentaplegic (Dpp), one of the TGF-β family members in *Drosophila*. Dpp was shown to influence the specification of the DAs and the operculum (Twombly et al., 1996; Deng and Bownes, 1997; Dobens et al., 2000; Peri and Roth, 2000). Partial loss-of-function alleles of *dpp* and/or Dpp pathway components lead to the production of eggs with a reduced operculum and mis-positioned DAs. Conversely, increasing the *dpp* levels causes an expansion of anterior eggshell structures (Twombly et al., 1996; Dobens et al., 2000; Ward and Berg, 2005). Recently, it has been shown that *brinker* (*brk*), a repressor of Dpp target genes (Campbell and Tomlinson, 1999; Jazwinska et al., 1999; Minami et al., 1999), is essential for DA formation (Chen and Schupbach, 2006).

In this study we deal with two aspects of Dpp signaling within the follicular epithelium: first, with the global function of Dpp in the Grk-dependent specification of all dorsal follicle cell fates, and second, with the interplay of Dpp and EGF signaling gradients in specifying distinct dorsal follicle cell fates.

MATERIALS AND METHODS

RNA in situ hybridizations and immunohistochemistry

In situ hybridization was performed as described by Tautz and Pfeifle (Tautz and Pfeifle, 1989). Antibodies: anti-Broad Z1 [mouse monoclonal, Developmental Studies Hybridoma Bank (DSHB); 1:100 dilution], anti-Fasciclin 3 (Fas3) (mouse monoclonal, DSHB; 1:50), anti-pMAD (rabbit polyclonal, 1:3000, gift of Dr Morata, Centro de Biologia Molecular, Madrid, Spain), anti-β-gal (rabbit polyclonal, MP Biomedicals; 1:750), anti-green fluorescent protein (GFP) (rabbit polyclonal, Molecular Probes; 1:3000), anti-Medea (1:1000) (Sutherland et al., 2003), anti-Grk (ID12, mouse monoclonal, DSHB; 1:100), Alexa Fluor-555-conjugated anti-mouse, Alexa Fluor-555-conjugated anti-rabbit, Alexa Fluor-488-conjugated anti-rabbit and Alexa Fluor-488-conjugated anti-mouse (Molecular Probes; 1:400).

Genetic mosaics in the follicular epithelium

All loss-of-function clones genetically marked by the absence of GFP were generated by the FRT/FLP recombination technique (Xu and Rubin, 1993). Adult females were heat shocked for 1 hour at 37°C and dissected after 4 days. The ovaries were then processed for antibody staining. The following stocks were used: tkv^{a12} *FRT40A(neo)/CyO*; Med^{13}*neo82B FRT/TM3, Sb*; brk^{M68} *FRT18A/FM7*; and *pip-lacZ*.

Cloning of *Drosophila sno* (*dSno*)

A CG7233 cDNA was amplified from a *Drosophila* ovarian cDNA library (Stroumbakis et al., 1994) using the following primers: Sno1 (5′-CTTATATTAAACCCAAC-3′) and Sno2 (5′-GCCGTCGGCAAA-

Institute of Developmental Biology, University of Cologne, Gyrhofstr.17, D-50931, Germany.

*Author for correspondence (e-mail: siegfried.roth@uni-koeln.de)

Accepted 23 March 2007

ATGCAAATGC-3′). This cDNA closely resembles dSnoI as described by Takaesu et al. (Takaesu et al., 2006). The 1360 bp amplified fragment was cloned in pCR-TOPO 2.1 and sequenced. A *Kpn*I and *Not*I fragment from pCR-TOPO-*dSno* was cloned into blueskript for making antisense RNA probes and into pUAST to produce transgenic lines.

Generating *dSno* mutants

Mutations in *dSno* were generated by imprecise excisions of the P-element insertion, l(2)Sh1402 (see Fig. S1 in the supplementary material). The breakpoints of the deletions were mapped by PCR. We uncovered a total of 17 different lines that had deletions in the *dSno* region and all were homozygous viable. One of the lines, $dSno^{174}$, was fine mapped and turned out to be a deletion removing CG7233 (see Fig. S1 in the supplementary material).

RESULTS

The Dpp gradient in the follicular epithelium is not influenced by Grk signaling

dpp is transcribed in anterior follicle cells during stage 8 to 10 of oogenesis (Twombly et al., 1996; Dobens et al., 2000). These cells secrete Dpp protein that forms an anterior-to-posterior gradient as suggested from the distribution of the Dpp signal transducer pMAD (Tanimoto et al., 2000) and the expression of the direct Dpp target gene, *dad-lacZ* (Tsuneizumi et al., 1997; Muzzopappa and Wappner, 2005) (Fig. 1A-F). When the anterior follicle cells flatten, this gradient moves closer to the oocyte where Grk is already asymmetrically localized (Fig. 1A-F). At stage 10A the follicle cell rearrangement is completed. Thinly stretched-out follicle cells cover the nurse cells [nurse cell follicle cells (NFCs)]. Tall follicle cells cover the oocyte [columnar follicle cells (CFCs)]. *dpp* transcription is largely restricted to the NFCs (Twombly et al., 1996; Dobens et al., 2000), whereas decreasing levels of pMAD can be detected in a five cell-wide stripe and *dad* expression in a four cell-wide stripe of anterior CFCs (Fig. 1C,F). At the dorsal side these CFCs are exposed to high levels of Grk signaling (Fig. 1C, dorsal view; Fig. 1F, lateral view). Because Dpp and Grk signaling function together in specifying dorsal follicle cell fates, it is possible that at stage 10A a crosstalk between the two pathways ensues that affects the cytoplasmic signal transducers or primary Dpp target genes. This might result in a dorsoventral (DV) asymmetry of nuclear pMAD and/or *dad* expression at stage 10A. However, these patterns are symmetric along the DV axis (Fig. 1C,F). The same was observed for the distribution of the common Smad Medea (data not shown) (Wisotzkey et al., 1998; Parker et al., 2004; Muzzopappa and Wappner, 2005). We conclude that at least with regard to high and medium signaling levels (see below) there is no influence of Grk on Dpp signaling and primary Dpp target gene expression. These observations are in variance with the suggestion that Dpp signaling is significantly enhanced in dorsal follicle cells (Araujo and Bier, 2000; Carneiro et al., 2006).

Dpp has a direct long-range function in specifying the DAs

At stage 10A the presumptive operculum cells occupy a triangular-shaped region positioned at the anterior-dorsal side of the CFCs. They express high levels of Fas3 (Fig. 1K) (Kose et al., 1997; Ward and Berg, 2005). The DAs are largely derived from cells expressing high levels of BR-C (Fig. 1G) (Deng and Bownes, 1997; Dorman et al., 2004; Ward and Berg, 2005). In the following we will refer to these cells as BR cells.

The posterior-most BR cells are approximately nine-cell rows away from the NFCs in which Dpp is expressed and *dad* expression and pMAD expand only to the fourth and fifth rows of CFCs, respectively. Therefore, it is possible that the function of *dpp* in DA specification is mediated via a secondary signal (Dobens et al., 2000). To address this question we produced large follicle cell clones mutant for *Med*, a common Smad shared by the activin and Dpp signaling pathways (Wisotzkey et al., 1998; Parker et al., 2004) and *thickveins* (*tkv*), the type I receptor specific for Dpp (Raftery and Sutherland, 1999; Parker et al., 2004). *Med* and *tkv* mutant clones gave identical results.

Follicle cell clones homozygous mutant for either Med^{13} or tkv^{a12} and localized in dorsal-anterior regions of the CFCs show downregulation of both Fas3 and BR-C in a cell-autonomous manner (Fig. 1H-J,L-N). In rare cases in which the clone borders are highly irregular, single Med^{+} cells can be found surrounded by *Med* mutant cells. These Med^{+} cells express normal levels of BR-C. In addition, large anterior clones do not prevent BR-C expression in wild-type (wt) cells positioned posterior to the clone (Fig. 1H, arrows). Thus, Dpp protein spreads beyond the region that lacks Dpp signaling components to induce BR-C expression. These data suggest that a Dpp gradient exists in stage 10A egg chambers that extends at least nine-cell rows from the source of *dpp* expression and patterns the dorsal chorion structures. It also implies that our pMAD and *dad-lacZ* stainings can only be used to detect high-to-medium levels of Dpp signaling in the follicular epithelium (Fig. 1C,F).

Grk requires Dpp to induce DV eggshell polarity

A certain portion of the eggs laid by females in which large clones of *Med* or *tkv* mutant follicle cells were induced (henceforth termed tkv^{-}/Med^{-} eggs) lack, as expected, both the operculum and the two DAs. Surprisingly, these eggs are totally symmetric along the DV axis with regard to their overall egg structure; i.e. the chorion imprints and the region surrounding the micropyle show no DV asymmetries (Fig. 1U; Fig. 2G,H). This suggests that Dpp is required to induce all aspects of DV eggshell polarity. The tkv^{-}/Med^{-} eggs closely resemble eggs in which the second round of Grk signaling and thus the induction of DV polarity fails to occur (Micklem et al., 1997; Newmark et al., 1997; Peri and Roth, 2000; Guichet et al., 2001) (Fig. 1T). This suggests that Dpp is essential for Grk to induce DV eggshell polarity.

Therefore, we wondered whether Dpp is essential for all aspects of DV Grk signaling. Besides induction of dorsal follicle cell types, Grk is also involved in establishing the embryonic DV axis by repressing *pipe* (*pip*) (Sen et al., 1998). *pip* codes for a sulfotransferase that causes the sulfation of an unknown extracellular matrix component essential for embryonic DV axis formation, but not for eggshell polarity. *pip* expression was analyzed in egg chambers carrying large Med^{13} or tkv^{a12} mutant follicle cell clones (Fig. 1O-R). To detect *pip* expression we used a *pip-lacZ* reporter construct that contains 3 kb of genomic DNA upstream of the *pip* transcriptional start site (M.T. and S.R., unpublished data). No change in *pip-lacZ* expression was detected. Thus, Dpp is essential for those aspects of Grk signaling that lead to establishment of DV eggshell polarity, but does not affect follicle cell patterning required for embryonic axis formation.

Anterior-most eggshell structures require Dpp, but not Grk, signaling

Margarits et al. have distinguished three regions of the operculum with distinct cell imprints: one directly surrounding the micropyle, a second extending from there to the DAs and a third occupying the area between the DAs (Fig. 2A,B) (Margarits et al., 1980). In ventral and lateral regions the operculum is separated from the remaining chorion by a raised structure, the collar (Fig. 2B, white

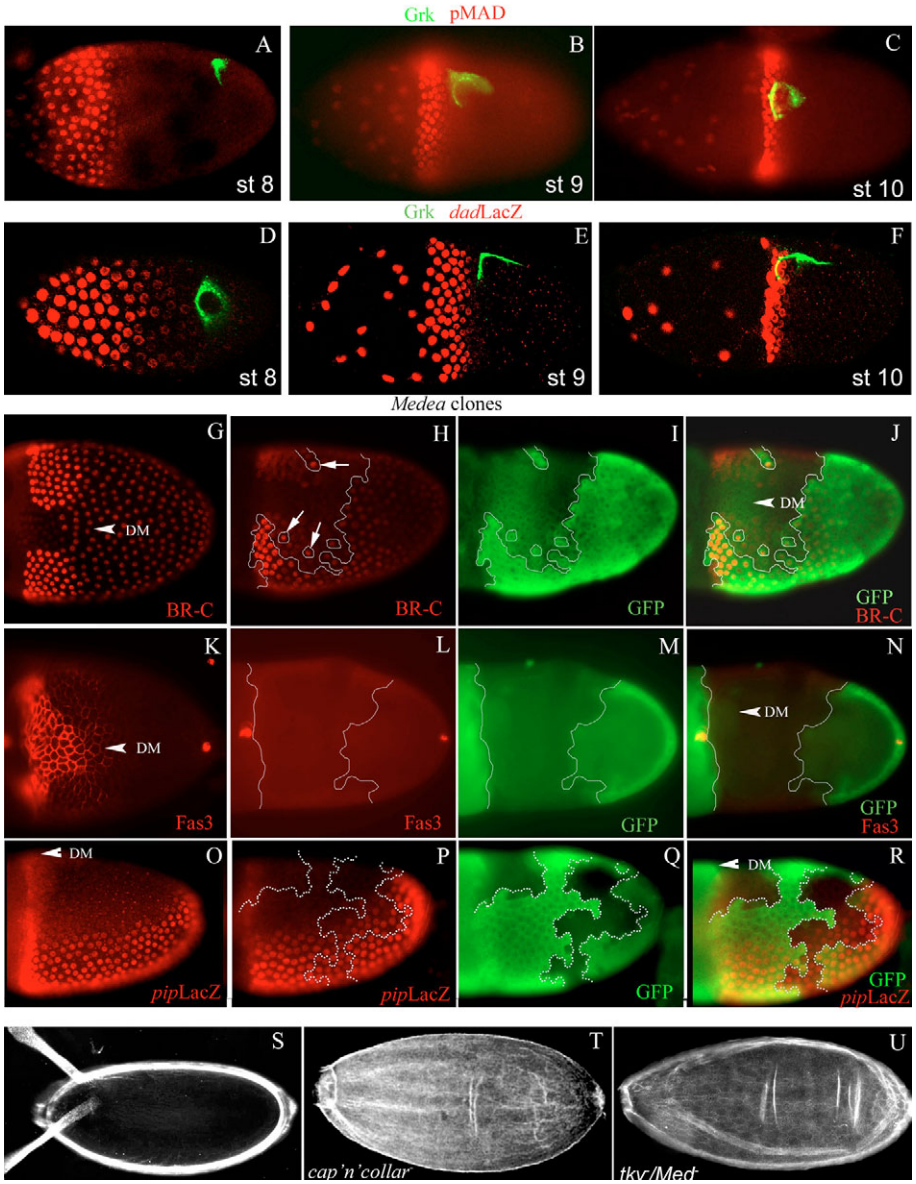

Fig. 1. Grk requires Dpp to induce DV eggshell polarity. Anterior is to the left. (**A-C**) Double immunofluorescence stainings for Grk (green) and pMAD (red). (A,B) Lateral views. (C) Dorsal view. (**D-F**) Double immunofluorescence stainings for Grk (green) and β-gal (red) of the egg chambers dissected from females carrying a *dad-lacZ* transgene. (D) Dorsal view. (E,F) Lateral views. (**G**,**K**) Immunofluorescence stainings for BR-C protein or Fas3 protein in wt stage 10B egg chambers; dorsal views. The white arrowheads mark the dorsal midline (DM). (**H-J**; **L-N**) Double immunofluorescence stainings for BR-C (red) or Fas3 (red) and GFP (green) in egg chambers carrying large Med^{13} mutant follicle cell clones; dorsal views. White lines mark the clone boundaries. White arrows in H mark single wt cells surrounded by cells mutant for Med^{13}. (**O**) Immunofluorescence staining for β-gal (red) of the egg chambers dissected from females carrying a *pipe-lacZ* transgene; lateral view. The white arrowhead marks the DM. (**P-R**) Double immunofluorescence stainings for β-gal (red) to detect *pipe-lacZ* and GFP (green) in egg chambers carrying large Med^{13} mutant follicle cell clones; lateral views. White lines mark the clone boundaries. (**S-U**) Darkfield micrographs of deposited eggs. (S) Wild-type egg. (T) Egg laid by female mutant for *cap-n-collar* (*cnc*) lacks DV eggshell polarity. In *cnc* mutants the oocyte nucleus is not anchored at the dorsal-anterior cortex of the oocyte. This prevents the induction of DV polarity by the second round of Grk signaling (Guichet et al., 2001). (U) Egg laid by female in which follicle cell clones mutant for Med^{13} were induced also lacks DV eggshell polarity.

arrow). In eggs derived from *grk* mutant females only regions II and III are deleted, whereas region I symmetrically surrounds the micropyle, followed by a symmetric collar (Fig. 2D,E). In Med^{-} eggs, in addition to the deletion of regions II and III, the chorionic region surrounding the micropyle is reduced in size and lacks chorion imprints, indicating that a particular follicle cell type is absent (Fig. 2G,H). In agreement with this assumption, both wt and *grk* mutant stage 14 egg chambers possess a group of follicle cells surrounding the micropyle that express high levels of Fas3 (Fig. 2C,F). This group of Fas3-positive cells is absent in tkv^{-}/Med^{-} eggs (Fig. 2I). Thus, Dpp apparently specifies the anterior-most region of the operculum in the absence of Grk signaling. This analysis also implies that only regions II and III of the operculum are true dorsal structures, whereas region I is an anterior structure.

We wondered whether Dpp is sufficient to specify region I of the operculum. To address this question we overexpressed Dpp in a *grk* mutant background using a GAL4 driver line that drives expression in all follicle cells (Queenan et al., 1997). *Grk* mutant eggs have micropyles at both ends, separated from the remaining chorion by a symmetric collar. Overexpression of *dpp* in a *grk* mutant background results in misshaped micropyles, the loss of the collar and a reduction of the egg diameter (Fig. 2J). These phenotypes were usually seen only at the egg pole, which harbors the nurse cells. They are accompanied by an expansion of the anterior Fas3 domain and patches of ectopic Fas3 expression in more central positions of the egg (Fig. 2K). Thus, Dpp overexpression in the absence of *grk* leads to the expansion of a follicle cell population that may correspond to region I of the operculum. In summary, these data suggest that Dpp is both required and sufficient to specify a subtype of anterior follicle cells in the absence of Grk signaling.

Combined overexpression of Grk and Dpp transforms all mainbody follicle cells into operculum fate and reveals a crosstalk between both pathways

To gain more information on how the two pathways interact in specifying different follicle cell types, we manipulated the levels of Dpp signaling within the follicular epithelium and at the same time increased the levels of Grk signaling from the oocyte.

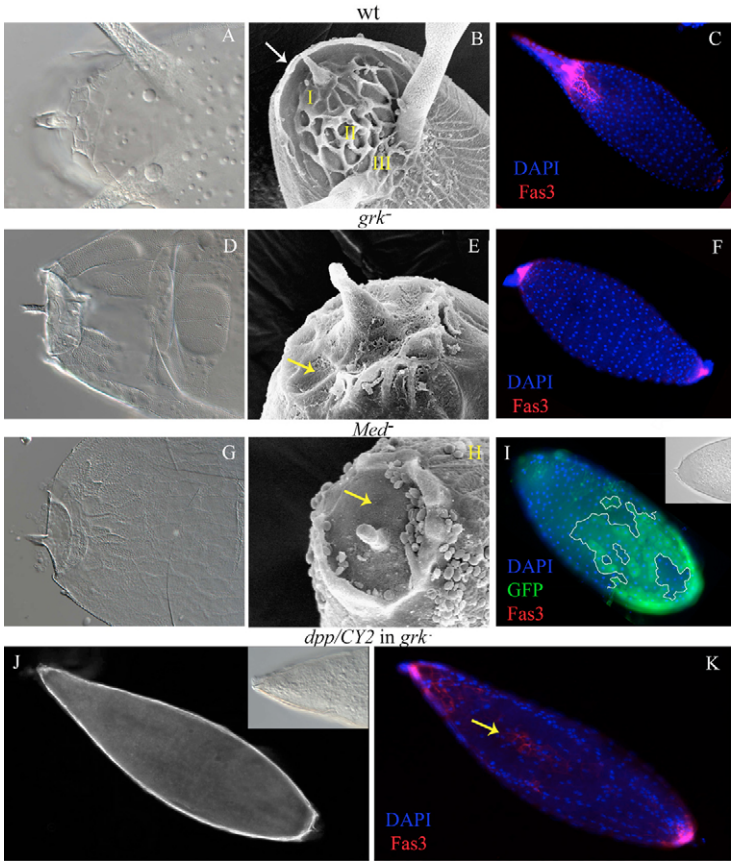

Fig. 2. Dpp is required for the anterior-most part of the operculum in the absence of Grk signaling. Anterior is to the left. (**A**,**D**,**G**) DIC micrographs of anterior eggshell regions. (**B**,**E**,**H**) SEM micrographs of anterior eggshell regions. (**C**,**F**,**I**,**K**) Stage 14 egg chambers stained for DAPI (blue) and Fas3 (operculum cells, red). (A-C) Wild-type. The operculum can be subdivided into three different regions (I, II, III). The white arrow marks the collar. (D-F) grk^{HF}/grk^{2B6} eggs have region I operculum cells surrounding the micropyle (yellow arrow) and stage 14 chambers show corresponding Fas3 expression. (G-I) In eggs from females carrying large *Med* mutant follicle cell clones the region surrounding the micropyle (yellow arrow) is reduced in size and lacks follicle cell imprints. (I) Med^{13} mutant follicle cell clones in a stage 14 egg chamber lack Fas3 expression. White lines mark the clone boundaries. The inset shows a DIC micrograph of the same egg demonstrating the integrity of the follicular epithelium at the anterior pole. Med^{13} mutant cell clones showed reduced levels of DAPI staining in later egg chambers. However, the integrity of the follicular epithelium was not affected. (J,K) Eggs and egg chamber from females misexpressing *dpp* in a grk^{HF}/grk^{2B6} background. (**J**) Darkfield micrograph of non-deposited egg (stage 15). Inset shows a DIC image of the abnormally thickened micropyle. (K) Stage 14 egg chamber. Fas3 expression is also found in random patches in more central positions of the main body follicle cells (marked by yellow arrow).

Two different Gal4 driver lines, GR1Gal4 and CY2Gal4, were utilized to drive moderate and high levels, respectively, of a UAS*dpp* transgene in all CFCs (Queenan et al., 1997; Goentoro et al., 2006). Moderate Dpp overexpresssion (GR1Gal4 × UAS*dpp*) leads to uniform pMAD levels in all follicle cells at stage 9 (data not shown), but levels decrease in early stage 10A (except for the posterior pole) and result in an extended gradient with randomly variegated pMAD levels (Fig. 3A). Higher levels of Dpp expression (Cy2Gal4 × UAS*dpp*) result in uniform levels of pMAD throughout stages 9 (data not shown) and 10A (Fig. 3B).

Grk overexpression was achieved using a maternal tub GAL4 driver line (Bökel et al., 2006). This driver line leads to a strong increase in the amount of Grk protein in stage 9 and 10 oocytes. The protein remains asymmetrically distributed, but higher concentrations are found at the ventral side compared with wt (compare Fig. 3C with Fig. 3A,B). Grk overexpression does not change the shape or anteriorposterior (AP) extension of the pMAD gradient (Fig. 3C), and combined overexpression of Grk and high amounts of Dpp results in the same uniform levels of pMAD expression as overexpression of Dpp alone (compare Fig. 3B with Fig. 3D). This confirms the assumption that Grk signaling does not influence the levels of Dpp signaling.

EGF signaling within the CFCs was monitored with the help of the primary EGF target gene *kekkon* (*kek*) (Queenan et al., 1997; Ghiglione et al., 1999; Peri and Roth, 2000; Guichet et al., 2001; Goentoro et al., 2006). In wt stage 10A egg chambers *kek* is expressed in a wedge-shaped domain of anterior-dorsal CFCs overlying the oocyte nucleus (Fig. 3Ed). It covers approximately 25% of the DV axis at the position of the nucleus and approximately 50% of the AP axis along the dorsal midline of the CFCs.

Moderate Dpp overexpression leads to eggs with enlarged DAs that are shifted towards posterior (Fig. 3Fa). Accordingly, the *BR-C* domains are dramatically enlarged, mainly by expanding towards posterior, whereas the lateral limits are only slightly shifted to the ventral side as compared with wt (Fig. 3Fc). Higher levels of Dpp expression lead to an expansion of the operculum at the expense of the DAs (Dobens et al., 2000) (Fig. 3Ga). *BR-C* expression is reduced to a narrow stripe encircling the expanded domain of Fas3 expression (Fig. 3Gb,c). Compared with moderate overexpression of *dpp*, the posterior and lateral limits of the total region giving rise to the dorsal follicle cells has only slightly changed. This region does not extend into the posterior-most 20% and is restricted to the dorsal-most 40% of the CFCs.

Surprisingly, *kek* expression expands laterally and posteriorly depending on the level of ectopic Dpp signaling (compare Fig. 3Ed with Fig. 3Fd and Fig. 3Gd). With Cy2Gal4 high levels of *kek* are found in a domain comprising 70% of AP and 40% of the DV axis. This expanded *kek* domain closely corresponds to the region that produces the enlarged operculum. If one assumes that *kek* expression directly reflects the levels of EGF signaling, this observation suggests that the activation of the Dpp pathway enhances the levels of EGF pathway activity.

The lateral borders of the region giving rise to dorsal follicle cells appear to be strictly defined by a certain threshold of Grk signaling. Increased Grk signaling leads to a ventral shift of the DA and an expansion of the operculum (Neuman-Silberberg and Schupbach, 1994) (data not shown). Strong Grk overexpression results in 30% of eggs with operculum as well as Fas3 expression along the entire DV axis, whereas BR-C transcription is

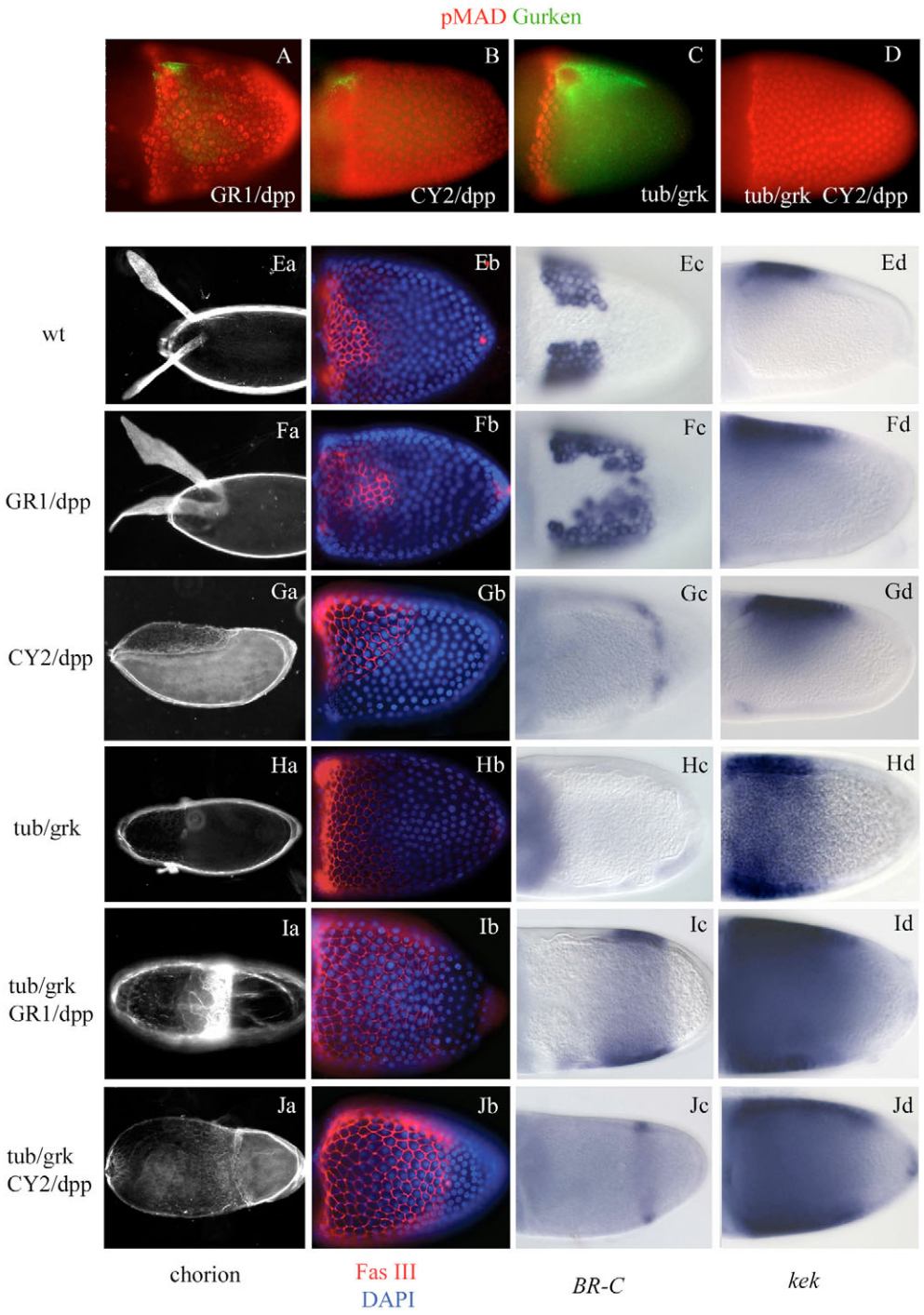

Fig. 3. Combined misexpression of Dpp and Grk transforms all mainbody follicle cells into dorsal follicle cells. Anterior is to the left. (**A-D**) Lateral views of stage 10 egg chambers. (A-C) Double immunofluorescence staining for Grk (green) and pMAD (red). (D) Immunofluorescence stainings for pMAD. (A) Moderate misexpression of *dpp* (UAS*dpp* × GR1-Gal4). (B) Strong misexpression of *dpp* (UAS*dpp* × CY2-Gal4). (C) Strong misexpression of *grk* (UASp*grk* × tub-Gal4VP16). (D) Simultaneous strong misexpression of *grk* (UASp*grk* × tub-Gal4VP16) and *dpp* (UAS*dpp* × CY2-Gal4). (**Ea-Ja**) Lateral view of darkfield micrographs of deposited eggs. (**Eb-Jb**) Immunofluorescence stainings for Fas3 (red) and DAPI (blue) of stage 10B egg chambers. Dorsal views, except in Gb, which shows a lateral view. (**Ec-Jc**) RNA in situ hybridization for *BR-C* on stage 10B egg chambers (dorsal view). (**Ed-Jd**) RNA in situ hybridization for *kek* on stage 10A egg chambers (lateral view) (Ea-d) Wild-type. (Fa-d) Moderate misexpression of *dpp* (UAS*dpp* × GR1-Gal4). (Ga-d) Strong misexpression of *dpp* (UAS*dpp* × CY2-Gal4). (Ha-d) Strong misexpression of *grk* (UASp*grk* × tub-Gal4VP16). (Ia-d) Strong misexpression of *grk* and moderate misexpression of *dpp*. (Ja-d) Strong misexpression of both *grk* and *dpp*.

suppressed (Fig. 3Ha-c). However, the AP width of the operculum and Fas3 expression are not altered. Accordingly, *kek* is expressed at high levels around the entire CFC circumference, although its expression remains restricted along the AP axis as in wt egg chambers (Fig. 3Hd). This is surprising because under the same conditions *pip* is repressed throughout the CFCs, indicating that Grk signals along the entire AP axis (Sen et al., 1998) (data not shown). This discrepancy is likely to be because of different thresholds of Grk signaling required for *kek* activation and *pipe* repression. We assume that even after strong Grk overexpression, high levels of EGF signaling remain restricted to the anterior half of the CFCs.

Upon simultaneous overexpression of Dpp and Grk, all columnar follicle cells are transformed into dorsal follicle cells with the exception of a cap of cells at the posterior pole (Fig. 3I,J). Moderate Dpp and strong Grk overexpression lead to a large anterior operculum followed by a symmetric band of DA material (Fig. 3Ia). Fas3 and BR-C are expressed in adjacent broad domains of similar width, which are symmetric along the DV axis (Fig. 3Ib,Ic). Strong overexpression of both Dpp and Grk results in an expansion of the operculum at the expense of the DA material (Fig. 3Ja). Correspondingly, the Fas3 domain is expanded at the expense of the BR-C domain (Fig. 3Jb,Jc). Again, these fate shifts are paralleled by an expansion of

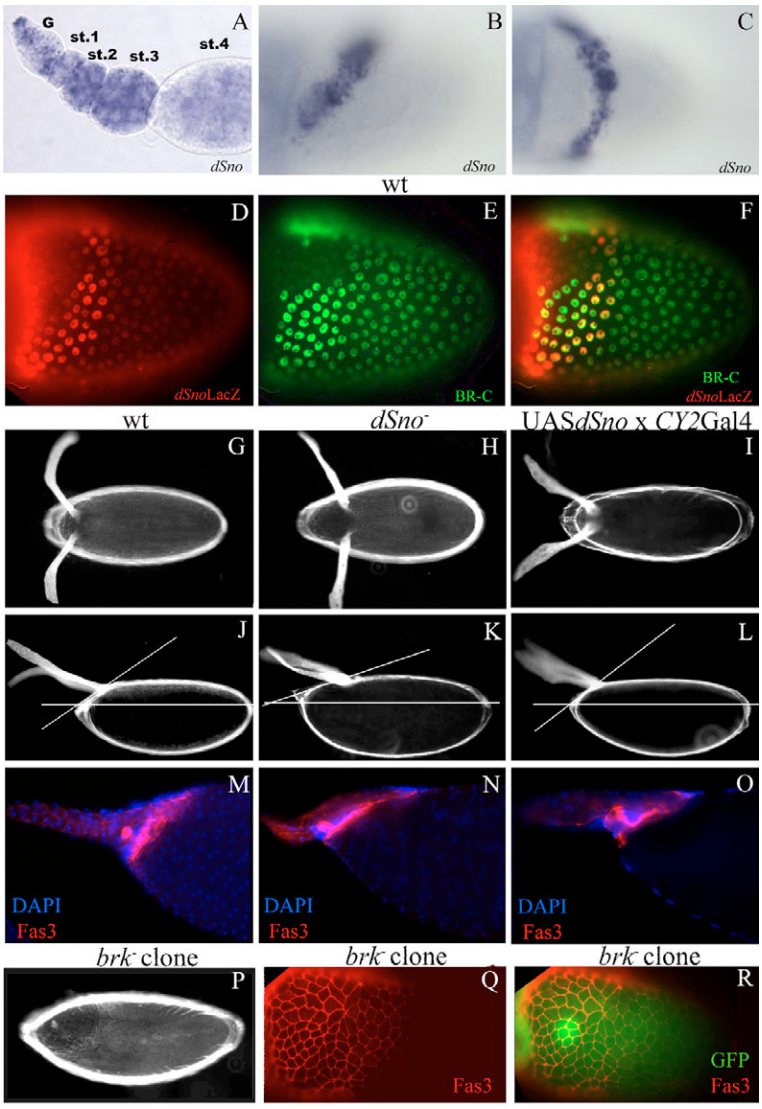

Fig. 4. Expression of *dSno* in ovaries and functional analysis of *dSno* and *brk*. Anterior is to the left. (**A-C**) RNA in situ hybridization for *dSno*. (A) Germarium and stage 1 to 4 egg chambers. (B) Lateral and (C) dorsal view of stage 10B egg chambers. (**D-F**) Double immunofluorescence for β-gal (red) and BR-C (green). *dSno-lacZ* is expressed at both lateral and posterior boundaries of the BR-C domain at stage 10B. (**G-I**) Dorsal view of darkfield micrographs of deposited eggs. (**J-L**) Lateral view of darkfield micrographs of deposited eggs. White lines serve to measure the operculum size. (**M-O**) Lateral view of stage 14 egg chambers stained for DAPI (blue) and Fas3 (red). (G,J,M) Wild-type. (H,K,N) $dSno^{174}/dSno^{174}$. (I,L,O) Overexpression of dSno (UAS*dSno* × CY2-Gal4). (**P**) Egg from female carrying large brk^{M68} mutant follicle cell clones. The DAs are replaced by an enlarged operculum. (**Q**,**R**) Double immunofluorescence stainings for Fas3 (red) and GFP (green) in a stage 10B egg chamber carrying a large dorsally located brk^{M68} mutant follicle cell clone.

the *kek* domain. Strong overexpression leads to uniform *kek* expression in all CFCs except for the posterior-most 20% (Fig. 3Jd).

Taken together, these data show that all CFCs, with the exception of the cells at the posterior pole, are competent to respond to a combination of Dpp and Grk by producing dorsal follicle cells. The refractory posterior cells are likely to correspond to the posterior terminal follicle cells that are unable to respond to the second round of Grk signaling (Gonzalez-Reyes and St Johnston, 1998; Peri and Roth, 2000). Within the region giving rise to dorsal follicle cells, high levels of Grk and high levels of Dpp have similar consequences: they promote operculum at the expense of the DA fates. A positive influence of Dpp signaling on the levels of EGF pathway activity might explain why both pathways are interchangeable with regard to certain cell fate decisions. Such a positive influence is suggested by changes of *kek* expression upon ectopic Dpp pathway activation. However, *kek* transcription is only an indirect indicator of EGF pathway activity, in contrast to, for example, the detection of activated MAPK. Thus, currently we cannot exclude alternative explanations for the observed effect of Dpp on *kek* expression. However, we favor a direct crosstalk between both pathways (see Discussion).

The functions of *dSno* and *brinker* in dorsal follicle cell patterning

To understand the read-out of the Dpp gradient we analyzed inhibitors of Dpp signaling and their interaction. In particular, we characterized the ovarian function of the *Drosophila* homolog of the Sno oncogene. *dSno* has recently been shown to antagonize TGF-β signaling in nervous system and in wing development (Takaesu et al., 2006; Ramel et al., 2007).

During ovarian development high levels of *dSno* are expressed at the tip of the germarium and lower levels in germline cells from stage 1 to stage 3 egg chambers (Fig. 4A). No obvious expression of *dSno* was observed from stage 4 to stage 9 (Fig. 4A and data not shown). Interestingly, at stage 10A *dSno* is expressed in a 3-4 cell-wide oblique stripe, which runs from an anterior-lateral to a posterior-dorsal position within CFCs (Fig. 4B,C; Fig. 5A). The *dSno* enhancer trap line, l(2)Sh1402 (Oh et al., 2003), reproduces this expression pattern and was used for colocalization studies (Fig. 4D-F). The posterior limit of *dSno* expression coincides with the posterior limits of the BR cells. Thus, the *dSno* stripe apparently encircles the entire follicle cell region, giving rise to dorsal chorion structures suggesting that it is involved in spatially limiting the range of Dpp signaling.

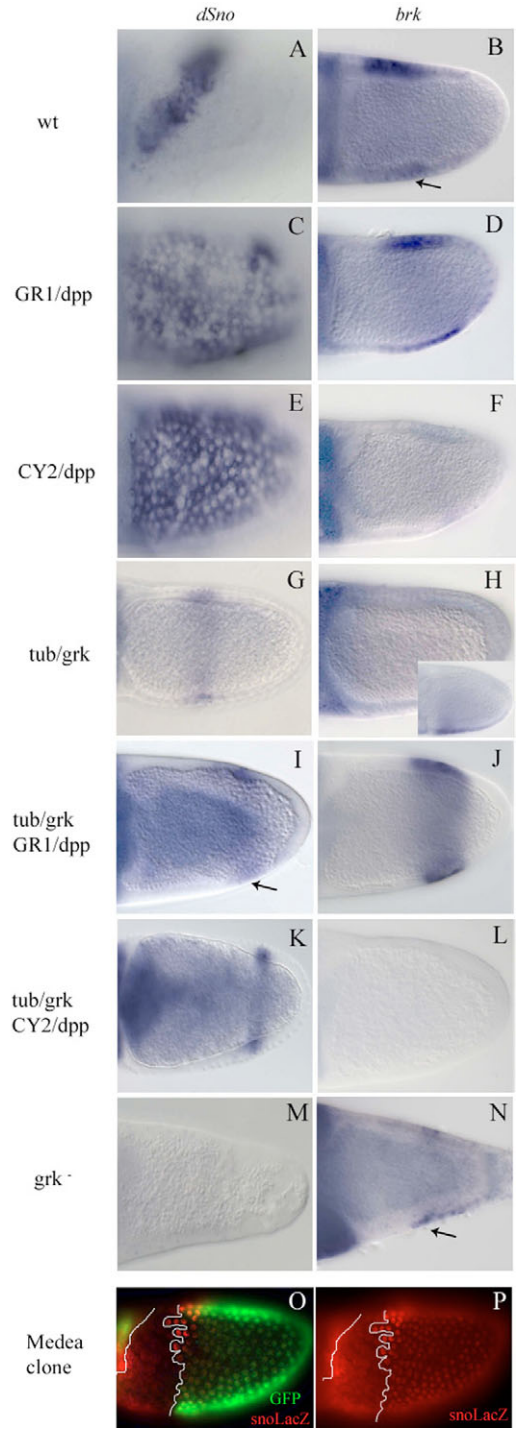

Fig. 5. Regulation of Dpp inhibitors by Grk and Dpp signaling. Anterior is to the left. Lateral view of stage 10B egg chambers. Only the posterior half of the egg chambers is shown. (**A**,**C**,**E**,**G**,**I**,**K**,**M**) RNA in situ hybridization for *dSno*. (**B**,**D**,**F**,**H**,**J**,**L**,**N**) RNA in situ hybridization for *brk*. The same genotypes are used as in Fig. 3. (A,B) Wild type. (C,D) Moderate misexpression of *dpp*. (E,F) Strong misexpression of *dpp*. (G,H) Strong misexpression of *grk*. Inset in H shows the shift of *brk* expression to the ventral follicle cells in moderate misexpression of *grk*. (I,J) Strong misexpression of *grk* and moderate misexpression of *dpp*. (K,L) Strong misexpression of *grk* and *dpp*. (M,N) grk^{HF}/grk^{2B6}. (**O**,**P**) Double immunofluorescence for β-gal (red) and GFP (green). *dSno* expression (*dSno-lacZ*) is downregulated cell autonomously in Med^{13} mutant follicle cell clones. White lines mark the clone boundaries.

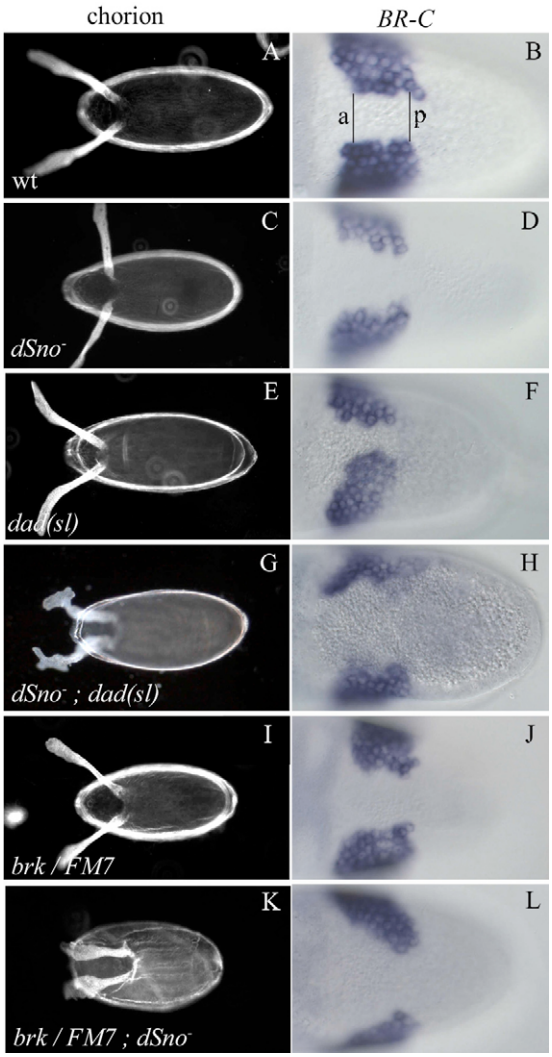

Fig. 6. *dSno*, *dad* and *brk* function redundantly in the follicular epithelium to inhibit Dpp signaling. Anterior is to the left. (**A**,**C**,**E**,**G**,**I**,**K**) Dorsal views of darkfield micrographs of deposited eggs. (**B**,**D**,**F**,**H**,**J**,**L**) Dorsal views of stage 10B egg chambers showing BR-C expression. (A,B) Wild type. (C,D) $dSno^{174}/dSno^{174}$. (E,F) *dad(sl)/dad(sl)*. (G,H) $dSno^{174}/dSno^{174}$; *dad(sl)/dad(sl)*. (I,J). brk^{M68}/+. (K,L) brk^{M68}/+; $dSno^{174}/dSno^{174}$.

To test this hypothesis we generated loss-of-function mutations in the *dSno* gene (see Materials and methods). $dSno^{174}$ is a 2.2 kb deletion that removes the domain of *dSno* essential for its interaction with Smad proteins in vertebrates (see Fig. S1 in the supplementary material). $dSno^{174}$ homozygous mutant flies are viable and produce viable progeny. However, a 50% reduction in viability was observed compared with wt. Also, the number of fertilized eggs was significantly decreased as compared with controls (65% as compared with 97% in control crosses). Interestingly, eggs deposited by $dSno^{174}/dSno^{174}$ females exhibit mild, but consistent patterning defects of dorsal chorion structures (Fig. 4H,K,N): the operculum is slightly enlarged and the DAs are shifted toward the posterior and are wider apart from each other and shorter than in wt eggs. Accordingly, the dorsal region between the BR-C domains is enlarged and the number of BR cells is decreased (Table 1; compare Fig. 6A,B with Fig. 6C,D). Overexpression of *dSno* using the strong driver line Cy2GAL4 leads to a reduction in

Table 1. *dSno* synergizes with *dad* and *brk*

	Number of BR cells	Anterior distance between the BR domains (a)	Posterior distance between the BR domains (p)
Wild type	52 (*n*=10; s.d. 2.85)	0.68 (*n*=7; s.d. 0.1)	0.54 (*n*=7; s.d. 0.03)
$dSno^{174}/dSno^{174}$	37 (*n*=13; s.d. 3.49)	1.16 (*n*=7; s.d. 0.22)	0.77 (*n*=7; s.d. 0.15)
dad(sl)/dad(sl)	49 (*n*=7; s.d. 4.85)	0.67 (*n*=7; s.d. 0.07)	0.59 (*n*=7; s.d. 0.06)
$brk^{M68}/+$	48 (*n*=7; s.d. 4.47)	1.15 (*n*=7; s.d. 0.15)	0.90 (*n*=7; s.d. 0.03)
$dSno^{174}/dSno^{174}$; *dad(sl)/dad(sl)*	41 (*n*=7; s.d. 8.02)	1.31 (*n*=7; s.d. 0.15)	1.22 (*n*=7; s.d. 0.3)
$brk^{M68}/+$; $dSno^{174}/dSno^{174}$	39 (*n*=7; s.d. 2.87)	1.63 (*n*=6; s.d. 0.08)	1.29 (*n*=6; s.d. 0.15)

The number of BR cells was determined from in situ hybridizations. The anterior and posterior distances were measured by drawing a straight line at the anterior and posterior boundaries of BR domains in Adobe Photoshop CS2, using the measuring tool (see Fig. 6B). The egg chambers from different mutant lines were treated in the same way and mounted on slides for microscopy, using spacers to prevent deformations.

the size of the operculum and a shift of the DAs towards anterior (Fig. 4I,L,O). Neither loss-of-function nor overexpression of *dSno* results in a change in *dpp* mRNA expression or pMAD distribution (see Fig. S2 in the supplementary material). Nevertheless, the loss-of-function phenotype of *dSno* is reminiscent of enhanced Dpp signaling, whereas the overexpression phenotype resembles reduced Dpp signaling. It is therefore likely that *dSno* acts directly or indirectly as a Dpp pathway inhibitor within the follicular epithelium.

Expression and function of *dSno* can be compared with that of *brk*, which has recently been shown to play a role in follicle cell patterning (Chen and Schupbach, 2006). *brk* is, like *dSno*, largely absent in the region giving rise to the operculum, but its expression shows more extensive overlap with the region giving rise to the DAs (Chen and Schupbach, 2006) (Fig. 5B). In addition, *brk* expression decreases towards the ventral side and lacks a sharp posterior boundary (Chen and Schupbach, 2006) (Fig. 5B). Like *dSno*, *brk* is also required to limit the size of the operculum. However, in contrast to *dSno*, loss of *brk* leads to a complete deletion of the DAs (Chen and Schupbach, 2006) (Fig. 4P-R). The operculum does not increase its AP dimension, but expands laterally at the expense of the DA anlagen. Large dorsally located *brk* clones lead to a broad dorsal domain of uniform Fas3 expression (Fig. 4Q,R).

dSno and *brinker* are dual targets of Dpp and EGF signaling in the follicular epithelium

Like vertebrate *sno*, *dSno* is activated by TGF-β signaling (Luo, 2004). This follows from cell clones mutant for *Med.* In such clones, in which Dpp signaling is abolished, *dSno* is not expressed (Fig. 5O,P). By contrast, *brk* has recently been shown to be repressed by Dpp signaling. Accordingly, strong overexpression of Dpp leads to uniform expression of *dSno*, whereas it completely abolishes *brk* expression (Fig. 5E,F). Mild overexpression of Dpp causes an irregular expansion of *dSno* expression and an enlargement of the anterior region of *brk* repression (Fig. 5C,D).

The regulation of *dSno* and *brk* expression by EGF signaling is complex. Egg chambers lacking Grk signaling do not express *dSno* (Fig. 5M). However, they show weak expression of *brk* in a central region of the CFCs (Fig. 5N). Thus, EGF signaling is required for *dSno*, but not for *brk* activation. Intermediate levels of EGF signaling seem to promote both *dSno* and *brk* expression whereas high levels repress both genes (compare Fig. 5A,G for dSno with Fig. 5B,H, including inset, for *brk*). Thus, in the case of *brk* mild EGF signaling counteracts the repressive effect of Dpp, whereas in the case of *dSno* mild EGF collaborates with Dpp. This subtle balance between Grk and Dpp signaling leads to the semi-circular expression domain in the case of *dSno*, whereas it provides a sharp anterior on-off boundary in the case of *brk*.

A paradoxical situation with regard to *brk* expression is observed upon mild overexpression of Dpp: Dpp appears to enhance rather than repress *brk* (Fig. 5D,J). However, given our observation that Dpp signaling promotes *kek* expression, suggesting that it enhances EGF signaling, these results can be explained by an indirect effect via EGF signaling: Dpp leads to additional EGF signaling and this, in turn, activates *brk*. With regard to *brk*, the regulatory input of EGF and Dpp signaling appears to be balanced such that *brk* expression always correlates with the formation of DAs.

Taken together, *brk* and *dSno* show similarities and differences in their regulation by Dpp and Grk. Therefore, they possess different, but partially overlapping, expression domains within the region giving rise to dorsal follicle cells. Moreover, the expression of both genes partially overlaps with *dad* expression (Fig. 1F). Dad is a negatively acting Smad protein (Tsuneizumi et al., 1997). The fact that *dSno* expression overlaps with that of two other Dpp inhibitors might explain its weak loss-of-function phenotype.

Dose-dependent interactions of Dpp inhibitors with *dSno*

To address this point we asked whether the homozygous *dSno* phenotype (compare Fig. 6C,D with Fig. 6A,B) was enhanced by removing one or two copies of the other inhibitors. Females homozygous for the semilethal P-insertion *dad(sl)* (Tsuneizumi et al., 1997) lay eggs that resemble wt eggs and show normal *BR-C* expression (compare Fig. 6E,F with Fig. 6A,B). Eggs laid by double homozygous $dSno^{174}$*; dad(sl)* mutants (Fig. 6G) have DAs that were thicker than those of *dSno* single mutants (compare with Fig. 6C) and had highly irregular ends in addition to an enlarged operculum. In accordance with this, the *BR-C* expression domains have irregular borders and are pushed laterally in stage 10B egg chambers (Fig. 6B,H). The dorsal distance between the BR-C domains is approximately twofold larger than in wt (Table 1).

We also generated a mutant line, which was homozygous for *dSno* and lacked one copy of *brk*. Eggs laid by such females are shorter in length and have a significantly larger operculum as compared with *dSno* homozygous or *brk* heterozygous mutants (Fig. 6C,I,K). Furthermore, the DAs are stout and massively thick at their ends (Fig. 6K) and *BR-C* expression is pushed more posteriorly and laterally (Fig. 6D,J,L; Table 1). Both in *dSno; dad(sl)* and in *brk; dSno* double mutants the number of BR cells is only slightly reduced. Thus, the massive expansion of the operculum does not occur at the expense of the DAs, but instead leads to lateral and posterior expansion of the total region giving rise to dorsal chorion fates. This suggests that *dSno* functions in concert with *dad* and *brk* in confining the region of the Dpp gradient that gives rise to dorsal chorion fates.

DISCUSSION

Our results show that Dpp has Grk-independent and Grk-dependent functions in the follicular epithelium. Even in the absence of Grk, Dpp is required to specify a group of anterior follicle cells that surround the micropyle (Fig. 2). All dorsal follicle cells that contribute to a morphologically visible polarization of the eggshell require the combined action of Grk and Dpp (Fig. 1U; Fig. 2G-I). Within the region giving rise to dorsal follicle cells, Dpp acts together with Grk in a concentration-dependent manner to specify the identity and position of at least two distinct follicle cell types.

Dorsoventral eggshell polarity strictly depends on Dpp

In the absence of Dpp, Grk can still activate *kekkon* (Peri and Roth, 2000; Guichet et al., 2001) and repress *pipe* (Fig. 1O-R). Thus, Dpp is not required for Grk signaling per se. We suggest that Dpp signaling rather activates transcription factors or causes chromatin modifications that allow Grk to induce dorsal target genes involved in follicle cell specification.

Mirror might be such a transcription factor that is activated by Dpp and confers the ability to adopt dorsal fates to a ring of anterior follicle cells (Jordan et al., 2000; Atkey et al., 2006). *mirror* acts downstream of Grk and probably also downstream of Dpp in specifying dorsal follicle cells (Atkey et al., 2006). However, *mirror* expression alone leads only to the formation of DA material. Thus, it is likely that *mirror* only provides the general potential to produce dorsal follicle cells. Additional inputs from Dpp and EGF signaling are needed to produce the full set of dorsal follicle cell fates. This scenario suggests two phases of Dpp signaling. An early phase demarcates the region in which Grk induces dorsal follicle cell fates. This might require only one (low level) threshold of Dpp signaling and is likely to be mediated through activation of *mirror*. A later phase establishes distinct dorsal follicle cell fates. Here, Dpp acts as a morphogen in combination with EGF signaling.

The correspondence of EGF signaling levels and dorsal follicle cell fates

The results presented in this study suggest that high levels of EGF and Dpp signaling correspond to regions II and III of the operculum, whereas lower levels of both pathways correspond to the DAs. With regard to region III of the operculum that separates the two DAs, our assumption appears to contradict the model of Wasserman and Freeman (Wasserman and Freeman, 1998). These authors showed that Grk signaling induces the expression of *rhomboid* (*rho*), which in turn activates Spitz, a second TGF-α-like molecule. This leads to an amplification of EGF signaling. Highest signaling levels centered at the dorsal midline lead to the induction of the inhibitor *argos* (*aos*), which antagonizes Spitz. This in turn lowers the levels of EGF signaling along the dorsal mildline. According to this model, high levels of EGF signaling promote DA, lower levels operculum region III formation. However, the expression patterns of *kek*, which result from Grk or Dpp overexpression, appear to contradict this model. Indeed, we believe that the regulatory loop of *rho* and *aos* is not required to establish the operculum or DA fates per se. The pattern of BR-C expression is not significantly altered in *rho* or *aos* mutant follicle cell clones (G.A., B.V.S. and S.R., unpublished data). However, *rho* and *aos* might contribute to patterning processes that are required for the morphogenesis and, as a result of this, for splitting of the DAs. Ward and Berg have shown that DA extension (tube formation) requires the collaboration of *rho*-expressing floor cells and BR-C-expressing roof cells (Ward and Berg, 2005). The

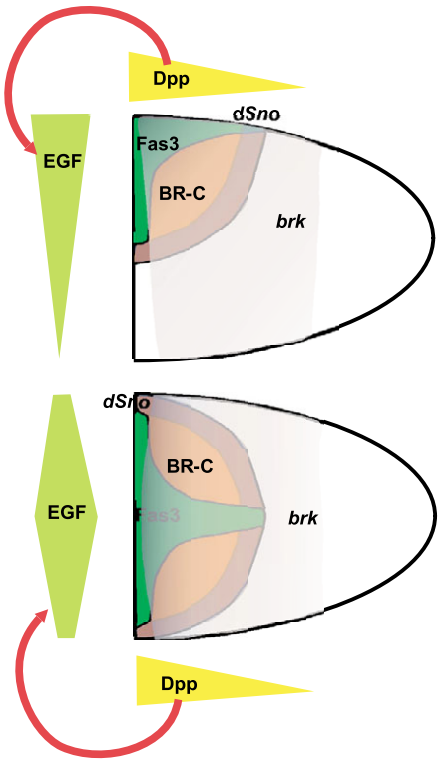

Fig. 7. Schematic representation of the signaling gradients and the expression domains of inhibitors involved in dorsal eggshell patterning.

rho-expressing floor cells are part of the Fas3 expression domain that separates the BR-C domains. These *rho*-expressing cells have to form a separate stripe on each side of the dorsal midline to allow the splitting of the DAs (Ward and Berg, 2005). We suggest that the *rho*/*aos* regulatory loop is required to generate two distinct stripes of late-*rho* expression within the dorsal Fas3 domain. The result is a splitting of the DAs accompanied by the establishment of a region of Fas3 cells that do not express *rho*, and thus give rise to region III of the operculum.

The read-out of the EGF and Dpp signaling gradients in the follicular epithelium and the functions of Dpp inhibitors

The establishment of the region giving rise to dorsal follicle cells and its subdivision into operculum and DA-producing cells is an intriguing problem of two-dimensional patterning (Fig. 7). The pattern of cell fates depends on the concentration-dependent read-out of two orthogonal signaling gradients (EGF and Dpp). This read-out is complex because the signaling pathways themselves appear to influence each other. First, there is evidence for a direct influence of Dpp on EGF signaling; second, the Dpp inhibitors *brk* and *dSno* are targets of both pathways; and third, *rho* is also a target of both pathways (Peri and Roth, 2000), an aspect that will not be further discussed here.

Evidence for a direct crosstalk between both pathways is provided by the analysis of *kek* expression. *kek* appears to be a primary target gene of EGF signaling as basal levels of its expression are independent of Dpp (Peri and Roth, 2000; Guichet et al., 2001). However, we observed an enhancement of *kek* expression upon *dpp* overexpression in stage 10A prior to the activation of *rho* and *aos*.

Moreover, the stage 10B expression patterns of *rho* and *aos* do not correlate with the observed changes in *kek* expression (data no shown). Thus, these changes cannot be caused by the secondary modulation of the EGF signaling profile. Therefore, we suggest a direct crosstalk between both pathways. This could be because of a Dpp receptor-dependent activation of the ras/MAPK cascade. A TGF-β receptor-dependent activation of the MAPK cascade has been observed in several vertebrate cell types (for reviews, see Derynck and Zhang, 2003; Javelaud and Mauviel, 2005). One could imagine that the triangular-shaped domain of Fas3 expression, which defines the anterior and dorsal borders of the BR-C domain, is specified by high levels of EGF signaling brought about by a Dpp-dependent enhancement of MAPK signaling. A confirmation of this model would necessitate direct monitoring of MAPK activity upon altered Dpp signaling.

The border between operculum and DAs is also crucially dependent on *brk*. In *brk* mutant follicle cell clones, Fas3 expression expands at the expense of the BR-C domains (Fig. 4P-R) (Chen and Schupbach, 2006). However, *brk* expression is upregulated within a broad domain at the dorsal side that also includes the Fas3-expressing region separating the BR-C domains (Fig. 5B). Although *brk* represses Fas3 expression in lateral regions allowing BR-C expression, *brk* is unable to repress Fas3 at the dorsal midline (Fig. 7). This suggests that Fas3 expression, which is predominantly dependent on high levels of EGF signaling, cannot be repressed by *brk*, whereas Fas3 expression in more lateral regions predominantly dependent on Dpp signaling is repressed by *brk*.

The hemi-circular boundary of the total region giving rise to dorsal chorion fates appears to be defined by a constant value reflecting the sum or the product of EGF and Dpp signaling (Fig. 7). The *cis*-regulatory elements of *dSno* represent a sensitive sensor for this dual input. At the dorsal midline, lower amounts of Dpp signaling are required to activate *dSno* than in lateral regions, and the opposite holds true for EGF signaling (Fig. 7). During brain development in flies (Takaesu et al., 2006) and in several contexts in vertebrates (for a review, see Luo, 2004) Sno is involved in the control of cell proliferation that has been shown to be crucially dependent on the relative levels of TGF-β and EGF signaling (for a review, see Siegel and Massague, 2003). It is conceivable that for spatial patterning of the follicular epithelium *dSno* uses regulatory elements that are derived from a more basic function in the control of cell proliferation in other tissues. The follicle cell expression of *dSno* might provide a convenient experimental setting to dissect such regulatory elements.

The fact that loss of *dSno* causes only mild defects is because of redundancy. A combination of three Dpp inhibitors appears to be involved in establishing the border between dorsal follicle cells and the remainder of the mainbody follicular epithelium. *brk* clones alone have no effect on the position of this border because they cause only a replacement of the DAs by operculum (Fig. 4P-R) (Chen and Schupbach, 2006). *dad* mutant clones seem to lack patterning defects altogether (Chen and Schupbach, 2006). However, already removing one copy of these inhibitors in a homozygous *dSno* mutant background leads to an enlargement of operculum and a posterior shift of the DAs. Weak phenotypic effects of *dSno* have recently been reported for wing vein formation (Ramel et al., 2007). Wing vein formation, too, represents a developmental context in which several Dpp inhibitors collaborate.

Molecular function of *dSno*

The *dSno* mutation we have generated deletes a highly conserved protein domain that is responsible for the interaction with Smad proteins in vertebrates (for a review, see Luo, 2004) and with Medea in flies (Takaesu et al., 2006). The knockout mutations in mice are based on the deletion of this domain (Shinagawa et al., 2000). Thus, this *dSno* mutation should represent a null allele. However, Takaesu et al. report an unusual complexity of the *dSno* locus and describe a deletion that suggests that *dSno* is lethal, in variance to our findings (Takaesu et al., 2006). However, Ramel et al. describe a truncation allele lacking an important part of the conserved Smad interaction domain that, like our allele, is viable (Ramel et al., 2007). Because the possibility exists that the deletion described by Takaesu et al. affects other genes in the chromosomal region of *dSno* (Takaesu et al., 2006), the question of lethality of *dSno* requires further analysis.

Loss of *dSno* in the follicular epithelium does not result in changes in *dpp* expression or pMAD distribution. Whereas a feedback on *dpp* expression was not expected, possible changes in pMAD distribution might be below the level of detection with our staining protocol. However, there are two other possible explanations. First, in brain development *dSno* has been shown to be a mediator of Baboon (Activin), rather than Dpp signaling (Takaesu et al., 2006). To investigate whether this also holds true for the follicular epithelium we have induced large *baboon* (Activin type I receptor) mutant follicle cell clones. These clones did not show patterning defects (data not shown), suggesting that *dSno* does not act via Baboon signaling with regard to follicle cell patterning. Second, the failure to detect changes in pMAD distribution might follow from the molecular mechanism of Sno action. A core feature of the inhibitory function of Sno proteins results from their ability to bind to the common Smad (Smad4). This binding prevents (or modulates) the interaction with phosphorylated R-Smads required for the transcriptional control of target genes (Wu et al., 2002). If this mechanism applies to DSno, the loss of *dSno* would not change the phosphorylation state of MAD and, if the interaction between DSno and Medea occurred predominantly in the nucleus, there would also be no significant change in the nuclear accumulation of pMAD.

We thank Michael Hoffman and Tetsuya Tabata for providing fly stocks, Laurel Raftery for the gift of anti-Medea antibodies, Gines Morata for the gift of anti-pMAD and Stuart Newfeld and Trudi Schupbach for communicating data prior to publication. We are grateful to Veit Riechman and Jeremy Lynch for critical reading of the manuscript. The work was supported by the International Graduate School in Genetics and Functional Genomics at the University of Cologne and the DFG (CRC 572).

Supplementary material

Supplementary material for this article is available at http://dev.biologists.org/cgi/content/full/134/12/2261/DC1

References

Araujo, H. and Bier, E. (2000). sog and dpp exert opposing maternal functions to modify toll signalling and pattern the dorsoventral axis of the Drosophila embryo. *Development* **127**, 3631-3644.

Atkey, M. R., Lachance, J. F., Walczak, M., Rebello, T. and Nilson, L. A. (2006). Capicua regulates follicle cell fate in the Drosophila ovary through repression of mirror. *Development* **133**, 2115-2123.

Berg, C. A. (2005). The Drosophila shell game: patterning genes and morphological change. *Trends Genet.* **21**, 346-355.

Bökel, C., Dass, S., Wilsch-Brauninger, M. and Roth, S. (2006). Drosophila Cornichon acts as cargo receptor for ER export of the TGFalpha-like growth factor Gurken. *Development* **133**, 459-470.

Campbell, G. and Tomlinson, A. (1999). Transducing the Dpp morphogen gradient in the wing of Drosophila: regulation of Dpp targets by brinker. *Cell* **96**, 553-562.

Carneiro, K., Fontenele, M., Negreiros, E., Lopes, E., Bier, E. and Araujo, H. (2006). Graded maternal short gastrulation protein contributes to embryonic dorsal-ventral patterning by delayed induction. *Dev. Biol.* **296**, 203-218.

Chen, Y. and Schupbach, T. (2006). The role of brinker in eggshell patterning. *Mech. Dev.* **123**, 395-406.

Deng, W. M. and Bownes, M. (1997). Two signalling pathways specify localised

expression of the Broad-Complex in Drosophila eggshell patterning and morphogenesis. *Development* **124**, 4639-4647.
Derynck, R. and Zhang, Y. E. (2003). Smad-dependent and Smad-independent pathways in TGF-beta family signalling. *Nature* **425**, 577-584.
Dobens, L. L. and Raftery, L. A. (2000). Integration of epithelial patterning and morphogenesis in Drosophila ovarian follicle cells. *Dev. Dyn.* **218**, 80-93.
Dobens, L. L., Peterson, J. S., Treisman, J. and Raftery, L. A. (2000). Drosophila bunched integrates opposing DPP and EGF signals to set the operculum boundary. *Development* **127**, 745-754.
Dorman, J. B., James, K. E., Fraser, S. E., Kiehart, D. P. and Berg, C. A. (2004). bullwinkle is required for epithelial morphogenesis during Drosophila oogenesis. *Dev. Biol.* **267**, 320-341.
Ghiglione, C., Carraway, K. L., 3rd, Amundadottir, L. T., Boswell, R. E., Perrimon, N. and Duffy, J. B. (1999). The transmembrane molecule kekkon 1 acts in a feedback loop to negatively regulate the activity of the Drosophila EGF receptor during oogenesis. *Cell* **96**, 847-856.
Goentoro, L. A., Yakoby, N., Goodhouse, J., Schupbach, T. and Shvartsman, S. Y. (2006). Quantitative analysis of the GAL4/UAS system in *Drosophila* oogenesis. *Genesis* **44**, 66-74.
Gonzalez-Reyes, A. and St Johnston, D. (1998). Patterning of the follicle cell epithelium along the anterior-posterior axis during Drosophila oogenesis. *Development* **125**, 2837-2846.
Guichet, A., Peri, F. and Roth, S. (2001). Stable anterior anchoring of the oocyte nucleus is required to establish dorsoventral polarity of the Drosophila egg. *Dev. Biol.* **237**, 93-106.
Javelaud, D. and Mauviel, A. (2005). Crosstalk mechanisms between the mitogen-activated protein kinase pathways and Smad signaling downstream of TGF-beta: implications for carcinogenesis. *Oncogene* **24**, 5742-5750.
Jazwinska, A., Kirov, N., Wieschaus, E., Roth, S. and Rushlow, C. (1999). The Drosophila gene brinker reveals a novel mechanism of Dpp target gene regulation. *Cell* **96**, 563-573.
Jordan, K. C., Clegg, N. J., Blasi, J. A., Morimoto, A. M., Sen, J., Stein, D., McNeill, H., Deng, W. M., Tworoger, M. and Ruohola-Baker, H. (2000). The homeobox gene mirror links EGF signalling to embryonic dorso-ventral axis formation through notch activation. *Nat. Genet.* **24**, 429-433.
Kose, H., Rose, D., Zhu, X. and Chiba, A. (1997). Homophilic synaptic target recognition mediated by immunoglobulin-like cell adhesion molecule Fasciclin III. *Development* **124**, 4143-4152.
Luo, K. (2004). Ski and SnoN: negative regulators of TGF-beta signalling. *Curr. Opin. Genet. Dev.* **14**, 65-70.
Margaritis, L. H., Kafatos, F. C. and Petri, W. H. (1980). The eggshell of Drosophila melanogaster. I. Fine structure of the layers and regions of the wild-type eggshell. *J. Cell Sci.* **43**, 1-35.
Micklem, D. R., Dasgupta, R., Elliott, H., Gergely, F., Davidson, C., Brand, A., Gonzalez-Reyes, A. and St Johnston, D. (1997). The mago nashi gene is required for the polarisation of the oocyte and the formation of perpendicular axes in Drosophila. *Curr. Biol.* **7**, 468-478.
Minami, M., Kinoshita, N., Kamoshida, Y., Tanimoto, H. and Tabata, T. (1999). brinker is a target of Dpp in Drosophila that negatively regulates Dpp-dependent genes. *Nature* **398**, 242-246.
Muzzopappa, M. and Wappner, P. (2005). Multiple roles of the F-box protein Slimb in Drosophila egg chamber development. *Development* **132**, 2561-2571.
Neuman-Silberberg, F. S. and Schupbach, T. (1993). The Drosophila dorsoventral patterning gene gurken produces a dorsally localized RNA and encodes a TGF alpha-like protein. *Cell* **75**, 165-174.
Neuman-Silberberg, F. S. and Schupbach, T. (1994). Dorsoventral axis formation in Drosophila depends on the correct dosage of the gene gurken. *Development* **120**, 2457-2463.
Newmark, P. A., Mohr, S. E., Gong, L. and Boswell, R. E. (1997). mago nashi mediates the posterior follicle cell-to-oocyte signal to organize axis formation in Drosophila. *Development* **124**, 3197-3207.
Nilson, L. A. and Schupbach, T. (1999). EGF receptor signalling in Drosophila oogenesis. *Curr. Top. Dev. Biol.* **44**, 203-243.
Oh, S. W., Kingsley, T., Shin, H. H., Zheng, Z., Chen, H. W., Chen, X., Wang, H., Ruan, P., Moody, M. and Hou, S. X. (2003). A P-element insertion screen identified mutations in 455 novel essential genes in Drosophila. *Genetics* **163**, 195-201.
Parker, L., Stathakis, D. G. and Arora, K. (2004). Regulation of BMP and activin signalling in Drosophila. *Prog. Mol. Subcell. Biol.* **34**, 73-101.
Peri, F. and Roth, S. (2000). Combined activities of Gurken and decapentaplegic specify dorsal chorion structures of the Drosophila egg. *Development* **127**, 841-850.
Queenan, A. M., Ghabrial, A. and Schupbach, T. (1997). Ectopic activation of torpedo/Egfr, a Drosophila receptor tyrosine kinase, dorsalizes both the eggshell and the embryo. *Development* **124**, 3871-3880.
Raftery, L. A. and Sutherland, D. J. (1999). TGF-beta family signal transduction in Drosophila development: from Mad to Smads. *Dev. Biol.* **210**, 251-268.
Ramel, M. C., Emery, C. S., Foulger, R., Goberdhan, D. C., van den Heuvel, M. and Wilson, C. (2007). Drosophila SnoN modulates growth and patterning by antagonizing TGF-beta signalling. *Mech. Dev.* **124**, 304-317.
Roth, S. (2003). The origin of dorsoventral polarity in Drosophila. *Philos. Trans. R. Soc. Lond. B Biol. Sci.* **358**, 1317-1329; discussion 1329.
Sen, J., Goltz, J. S., Stevens, L. and Stein, D. (1998). Spatially restricted expression of pipe in the Drosophila egg chamber defines embryonic dorsal-ventral polarity. *Cell* **95**, 471-481.
Shinagawa, T., Dong, H. D., Xu, M., Maekawa, T. and Ishii, S. (2000). The sno gene, which encodes a component of the histone deacetylase complex, acts as a tumor suppressor in mice. *EMBO J.* **19**, 2280-2291.
Siegel, P. M. and Massague, J. (2003). Cytostatic and apoptotic actions of TGF-beta in homeostasis and cancer. *Nat. Rev. Cancer* **3**, 807-821.
Spradling, A. C. (1993). Development genetics of oogenesis. In *The Development of Drosophila melanogaster* (ed. M. Bate and A. Martinez-Arias), pp. 1-70. Cold Spring Harbor: Cold Spring Harbour Laboratory Press.
Stroumbakis, N. D., Li, Z. and Tolias, P. P. (1994). RNA- and single-stranded DNA-binding (SSB) proteins expressed during Drosophila melanogaster oogenesis: a homolog of bacterial and eukaryotic mitochondrial SSBs. *Gene* **143**, 171-177.
Sutherland, D. J., Li, M., Liu, X. Q., Stefancsik, R. and Raftery, L. A. (2003). Stepwise formation of a SMAD activity gradient during dorsal-ventral patterning of the Drosophila embryo. *Development* **130**, 5705-5716.
Takaesu, N. T., Hyman-Walsh, C., Ye, Y., Wisotzkey, R. G., Stinchfield, M. J., O'Connor, M. B., Wotton, D. and Newfeld, S. J. (2006). dSno facilitates baboon signaling in the Drosophila brain by switching the affinity of Medea away from Mad and toward dSmad2. *Genetics* **174**, 1299-1313.
Tanimoto, H., Itoh, S., ten Dijke, P. and Tabata, T. (2000). Hedgehog creates a gradient of DPP activity in Drosophila wing imaginal discs. *Mol. Cell* **5**, 59-71.
Tautz, D. and Pfeifle, C. (1989). A non-radioactive in situ hybridization method for the localization of specific RNAs in Drosophila embryos reveals translational control of the segmentation gene hunchback. *Chromosoma* **98**, 81-85.
Tsuneizumi, K., Nakayama, T., Kamoshida, Y., Kornberg, T. B., Christian, J. L. and Tabata, T. (1997). Daughters against dpp modulates dpp organizing activity in Drosophila wing development. *Nature* **389**, 627-631.
Twombly, V., Blackman, R. K., Jin, H., Graff, J. M., Padgett, R. W. and Gelbart, W. M. (1996). The TGF-beta signalling pathway is essential for Drosophila oogenesis. *Development* **122**, 1555-1565.
Ward, E. J. and Berg, C. A. (2005). Juxtaposition between two cell types is necessary for dorsal appendage tube formation. *Mech. Dev.* **122**, 241-255.
Wasserman, J. and Freeman, M. (1998). An autoregulatory cascade of EGF receptor signaling patterns the Drosophila egg. *Cell* **95**, 355-364.
Wisotzkey, R. G., Mehra, A., Sutherland, D. J., Dobens, L. L., Liu, X., Dohrmann, C., Attisano, L. and Raftery, L. A. (1998). Medea is a Drosophila Smad4 homolog that is differentially required to potentiate DPP responses. *Development* **125**, 1433-1445.
Wu, J. W., Krawitz, A. R., Chai, J., Li, W., Zhang, F., Luo, K. and Shi, Y. (2002). Structural mechanism of Smad4 recognition by the nuclear oncoprotein Ski: insights on Ski-mediated repression of TGF-beta signalling. *Cell* **111**, 357-367.
Xu, T. and Rubin, G. M. (1993). Analysis of genetic mosaics in developing and adult Drosophila tissues. *Development* **117**, 1223-1237.